A measure of the DNA barcode gap for applied and basic research

Jarrett D Phillips, Cortland K Griswold, Robert G Young, Nicolas Hubert, Robert H Hanner

A measure of the DNA barcode gap for applied and basic research

Jarrett D. Phillips[1,4‡*] (ORCID: 0000-0001-8390-386X),
Cortland K. Griswold[4‡] (ORCID: 0000-0003-2993-7043)
Robert G. Young[4] (ORCID: 0000-0002-6731-2506)
Nicolas Hubert[2] (ORCID: 0000-0001-9248-3377)
Robert H. Hanner[3,4] (ORCID: 0000-0003-0703-1646)

[1]*School of Computer Science, University of Guelph, Ontario, Canada N1G 2W1*
[2]*UMR ISEM (IRD, UM, CNRS), Université de Montpellier, Place Eugène Bataillon, 34095 Montpellier cedex 05, France*
[3]*Biodiversity Institute of Ontario, University of Guelph, Ontario, Canada N1G 2W1*
[4]*Department of Integrative Biology, University of Guelph, Ontario, Canada N1G 2W1*

[‡] Equal contribution

*__Correspondence__: Jarrett D. Phillips
__Email__: jphill01@uoguelph.ca

__Keywords__: bootstrapping, DNA barcoding, intraspecific genetic distance, interspecific genetic distance, multispecies coalescent, nonparametrics, speciation

__Running Title__: A method to detect DNA barcode gaps

Abstract

DNA barcoding has largely established itself as a mainstay for rapid molecular taxonomic identification in both academic and applied research. The use of DNA barcoding as a molecular identification method depends on a "DNA barcode gap" — the separation between the maximum within-species difference and the minimum between-species difference. Previous work indicates the presence of a gap hinges on sampling effort for focal taxa and their close relatives. Furthermore, both theory and empirical work indicate a gap may not occur for related pairs of biological species. Here, we present a novel evaluation approach in the form of an easily calculated set of nonparametric metrics to quantify the extent of proportional overlap in inter- and intraspecific distributions of pairwise differences among target species and their conspecifics. The metrics are based on a simple count of the number of overlapping records for a species falling within the bounds of maximum intraspecific distance and minimum interspecific distance. Our approach takes advantage of the asymmetric directionality inherent in pairwise genetic distance distributions, which has not been previously done in the DNA barcoding literature. We apply the metrics to the predatory diving beetle genus *Agabus* as a case study because this group poses significant identification challenges due to its morphological uniformity despite both

relative sampling ease and well-established taxonomy. Results herein show that target species and their nearest neighbour species were found to be tightly clustered, and therefore difficult to distinguish. Such findings demonstrate that DNA barcoding can fail to fully resolve species in certain cases. Moving forward, we suggest the implementation of the proposed metrics be integrated into a common framework to be reported in any study that uses DNA barcoding for identification. In so doing, the importance of the DNA barcode gap and its components on the success of DNA-based identification using DNA barcodes can be better appreciated.

Introduction

The utility of DNA barcodes ***(1, 2)*** to provide species-level identifications to unknown specimens depends strongly on historical, geographical, and ecological processes shaping mitochondrial DNA (mtDNA) polymorphism ***(3, 4)***. Current identification based on DNA sequences further depends on the comprehensiveness of genomic sequence libraries housed in databases such as the Barcode of Life Data Systems (BOLD) (http://www.barcodinglife.org; ***(5)***) and GenBank (https://www.ncbi.nlm.nih.gov/genbank). In addition, the successful use of such data assumes sequencing, as well as species labelling, are error-free.

Despite access to over 12 million DNA barcodes across more than 340 thousand multicellular species in BOLD as of February 2023, current specimen sampling efforts are likely not sufficient to enable accurate taxonomic assignment of many sequences, as a majority species are still missing, and oftentimes less than 10 individuals (typically comprising only singletons) have been sampled for a species ***(6)***.

Having a broad representation of within-species genetic diversity is necessary when it comes to elucidating genetic species boundaries and to accurately estimate the DNA barcoding gap — the difference between maximum intraspecific and minimum (nearest neighbour) interspecific sequence variation ***(7, 8)***. Empirical observation inferred from marker-specific variation suggests intraspecific distances do not usually exceed those found among species, thereby indicating DNA sequences aptly capture the evolutionary genetic boundaries of species ***(1, 2)***. The existence of the DNA barcode gap has been invoked as the primary explanation for why DNA barcoding works well in practice; however, it has been demonstrated to fail in (population genetic) theory ***(9, 10, 11)***. In fact, several studies have suggested that DNA barcoding gaps can be an artifacts of insufficient specimen sampling, particularly across biological space (see ***(12)*** for some taxon-specific examples). With greater spatial coverage, intraspecific distances increase as a

result of isolation-by-distance, whereas interspecific distances tend to shrink due to encountering more closely related species ***(13)***. While much work has been devoted to assessing patterns of intraspecific variation using DNA barcodes and highlighting the importance of specimen sampling for reliable DNA barcode gap estimation ***(12)***, the role of interspecific genetic diversity on the success of DNA-based taxon identification has attracted less attention. Early on in DNA barcoding, barcode gaps were calculated using the mean intraspecific and mean interspecific genetic distance ***(7)***. However, this scheme was prone to exaggerating the width of gaps, leading to poor species delimitation and resolution of taxon boundaries. False positives in the form of taxonomic oversplitting (where the minimum interspecific distance falls below the maximum intraspecific distance), and false negatives manifesting as excessive species lumping (where the nearest neighbour distance lies above the maximum intraspecific distance), were common ***(7, 12)***. Later arguments for the use of the maximum intraspecific distance and the minimum interspecific distance greatly reduced identification biases in threshold-based species delimitation, but did not eliminate them altogether ***(8)***. Further, problems arise from the reporting of the DNA barcode gap, particularly in taxon reference library publications, where it is often treated as a binary (Yes/No) response, rather than as a continuous random variable with

measurable statistical error reflecting the overall extent of intraspecific and interspecific distribution overlap. Robust sampling is therefore necessary to reliably detect DNA barcode gaps when they actually exist ***(12)***.

Several computational and statistical approaches, in both parametric (model-based) and nonparametric (data-driven) settings, have been proposed to address the proper use of DNA barcodes. Tools for specimen identification and species delimitation include both frequentist likelihood and Bayesian posterior estimation models fitted via Markov Chain Monte Carlo (MCMC), for instance ***(14, 15)***. Taxon delineation methods like the Generalized Mixed Yule Coalescent (GMYC) ***(16)***, Automatic Barcode Gap Discovery (ABGD) ***(17)***, Poisson Tree Processes (PTP) ***(18)***, the Barcode Index Number (BIN) system ***(19)***, and Assemble Species by Automatic Partitioning (ASAP) ***(20)*** have seen extensive use as stand-alone tools for species delineation tasks (*e.g.*, the *splits* (Species LImits by Threshold Statistics) R package ***(21)***, as well as various webservers), despite numerous computational, statistical, and interpretational challenges ***(12)***. Often, the plethora of available methods for specimen identification and species delimitation tasks produces conflicting results when applied across the same dataset, making the selection of a single method daunting for end users.

Generally, specimen identification using DNA barcodes is routine whenever species boundaries delimited using standardized loci such as cytochrome *c* oxidase subunit I (COI) are concordant with those inferred from the examination of morphological characters. Despite DNA barcoding's strong presence and widespread use over the past two decades, what appears to still be missing is an automatic multi-use tool to assess genomic markers for downstream specimen identification. While consensus largely exists regarding marker choice for multicellular eukaryotic taxa like animals, plants, and fungi, the same cannot be said for unicellular and prokaryotic organisms such as protists and cyanobacteria, where a multimarker approach is likely required for accurate DNA barcode gap assessment (*e.g.*, ***(22, 23)***). This makes the development of such a marker evaluation scheme imperative.

In this paper, we propose statistical metrics to evaluate the DNA barcode gap based on coalescent theory ***(24)***, whose deep role in DNA-based species delimitation was previously noted by Hubert and Hanner ***(25)*** and applied using the multispecies coalescent (MSC) ***(26, 27)***. The application of the MSC in a multilocus context to help resolve instances of mixed haplotype clusters arising from non-monophyly was also previously advocated for by Collins and Cruickshank ***(28)***. They argued that multilocus MSC approaches provide stronger biological support for speciation events between sister taxon

pairs compared to simpler distance-based heuristics. Here, easily computed nonparametric statistics are proposed to measure the separation between intraspecific and interspecific sequence variation between pairs of species. They are relatively straightforward to implement and evaluate.

DNA Barcode Gap Metrics

Define the proposed DNA barcode gap metrics as follows:

$$p_x = \frac{\#\{d_{ij} \geq \min d_{XY}\}}{\#\{d_{ij}\}} \qquad (1),$$

$$q_x = \frac{\#\{d_{XY} \leq \max d_{ij}\}}{\#\{d_{XY}\}} \qquad (2).$$

where d_{ij} are intraspecific differences, d_{XY} are interspecific differences and # corresponds to the "Number of". Note in traditional estimation of the DNA barcode gap, the distribution of interspecific distances *excludes* the target species. In contrast, the present approach deviates from this by including *all* pairwise interspecific distances across all species pairs. The justification for employing this scheme is that it more accurately accounts for all species' and coalescent histories in the available sample of DNA sequences. Note, p_x and q_x are calculated for each species (x), such that $\#\{d_{ij}\}$ is the number of pairwise differences for a particular species and max d_{ij} is for a given species. See **Table 1** for a complete set of definitions.

[**Fig. 1** near here]

[**Fig. 2** near here]

[**Table 1** near here]

Equations (1) and (2) above express the degree of proportional overlap of intraspecific and interspecific genetic distance distributions. The metrics can be applied to either differentiate species at the genus level, or resolve separation of target taxa and their nearest neighbours (*i.e.*, sister species) within a genus of interest. For example, *XY* would cover either an entire genus, with each species being well sampled, or the nearest neighbour species. The quantity p_x measures the overlap of intraspecific differences with interspecific ones, whereas q_x measures the overlap of interspecific differences with intraspecific ones. To distinguish metrics for nearest neighbours, we add a prime symbol (') to p_x and q_x. The proposed metrics outlined here stand in sharp contrast to previous ones which only examine "average" effects at the "community" level. While we here apply the metrics at the species level, they are easily extended to the level of Operational Taxonomic Units (OTUs) and other similar species proxies. **Figures 1** and **2** motivate the statistics. In **Figure 1**, the quantity t_{AB} corresponds to the time species *A* and *B* formed. $t_{XY,\ \min}$ is the (unobserved) minimum divergence time for two mitochondrial genes from different species within the genus. $t_{ij,\ \max}$ is the (unobserved) maximum divergence time for two mitochondrial genes from individuals of the same

199 species across the entire genus. The Most Recent Common Ancestor (MRCA) of
200 the sample is noted, but in principle, the maximum (unobserved) divergence
201 time between species *A* and *B* ($t_{AB,\,\max}$) may be further back in time. **Figure 2**
202 relates times in **Figure 1** to the proposed statistics, and the distributions of
203 intraspecific and interspecific distances.

204 Quantities p_x and q_x (as well as p_x‘ and q_x‘) are bounded between zero
205 and one. Values near or equal to zero suggest evidence of species’ DNA
206 barcode gaps within the genus under consideration for a given sample and
207 species identifications. Conversely, values near or equal to one indicate little
208 to no evidence of species’ DNA barcode gaps, and therefore lack of support for
209 specimen assignment to species. Distances may be measured using, for
210 example, *p*-distance, Jukes-Cantor (JC69) ***(29)*** or Kimura-Two-Parameter
211 (K2P) models ***(30)***. More specifically, p_x and q_x are calculated through
212 counting the number of specimen record distances lying within the bounds for
213 intraspecific and interspecific comparisons and then dividing this sum by the
214 total number of considered distances, respectively. It should be noted that p_x
215 and q_x, as well as p_x‘ and q_x‘, are calculated herein using a hybrid approach
216 based on both the mean and the smallest intraspecific distance (see next
217 section). While the use of the minimum is more common than the mean in the
218 DNA barcoding literature, it is susceptible to specimen assignment errors in

BOLD and GenBank. Nevertheless, while the minimum interspecific distance can more easily expose cases of DNA barcode sharing, in well sampled taxa identified using highly diagnosable gene markers, phenomena such as introgressive hybridization still do occasionally occur.

A logical next step is testing for statistical significance and assessing deviations from expectations for a particular hypothesis. The proposed metrics are associated with considerable uncertainty given low sample sizes for most taxa within DNA barcode libraries. Thus, calculation of standard errors (SEs), which can be estimated through nonparametric bootstrapping ***(31)*** for instance, provided sample sizes are sufficiently large, is necessary. In cases where sample sizes are small however, no amount of bootstrapping will help ameliorate uncertainty, and if applied naively, give a false assessment of certainty ***(12)***, especially when the metrics are found to be equal to zero. Bootstrapping distances will not be informative in such cases. A more robust bootstrapping approach in the context of estimating the true degree of distribution overlap entails resampling alignment sites directly, like is done in phylogenetics, as opposed to distances themselves. Because a distance is already a summary over a set of sites, resampling nucleotide positions has the advantage of retaining more information given DNA barcode sequences are short in length. Thus, bootstrapping at the level of sites may be more

239 informative because, in principle, sites leading to no overlap may not be
240 included and an overlap may arise. In fact, because genetic distances used in
241 calculating the proposed metrics are not statistically independent and
242 identically distributed (IID) ***(12)***, estimator SEs will depend directly on the
243 number of sampled species within the focal genus (*K*), as well as indirectly on
244 the number of sampled specimens per species (*N*). Therefore, plots of the
245 proposed metrics *versus* their estimated SEs could be informative. In this
246 regard, considering two species, one well sampled, and the other poorly
247 sampled, the lower values of the proposed metrics will likely produce larger
248 SEs for the well-sampled species when its sample size is downsized to that of
249 the poorly sampled species. Appropriate (1 – α)100% confidence intervals for
250 the "true" DNA barcode gap metrics are also easily constructed, where α is the
251 desired significance level cutoff (*e.g.*, α = 0.05 for 95% confidence).
252
253 **Case Study: *Agabus* Diving Beetles (Coleoptera: Dytiscidae)**
254 We use the predaceous diving beetle genus *Agabus* (Coleoptera:
255 Dytiscidae), as a test case, which was previously examined by Bergsten *et al.*
256 ***(13)*** in the context of assessing the scale of geographic sampling on DNA
257 barcoding. *Agabus* consists of 199 named Linnaean species according to the
258 Global Biodiversity Information Facility (GBIF). DNA sequences for COI-5P,

COI-3P, and CYTB were automatically downloaded from GenBank and BOLD, aligned to reference sequences for *Agabus bipustulatus*, and cleaned on November 1, 2022 with the R package *MACER* (Molecular Acquisition, Cleaning and Evaluation in R) using default parameters ***(32)***. Data processing included removing sequences with ambiguous and/or missing nucleotide data (which was handled using pairwise deletion), omitting sequences containing sequencing artifacts such as stop codons, and excluding genus- and species level outliers (through use of the 1.5 × IQR (interquartile range) rule to discard taxon records having excessively divergent distance values). Aside from being well-represented within BOLD and GenBank, gene markers investigated were specifically selected due to their high representativeness in *Agabus*, widespread use in the DNA barcoding literature, as well as centrality in studies of phylogenetics and molecular evolution. All statistics were computed in R ***(33)*** using *p*-distances and integrated within *MACER*. Nonparametric bootstrap 95% percentile confidence intervals for the population means of p_x, q_x, p_x', and q_x' across all species for each marker were calculated with 10000 replications where possible using the *boot* R package ***(34, 35)***. In computing p_x', and q_x', it was not uncommon for focal taxa to be equally distant to multiple nearest neighbours based on the minimum interspecific distance. In such cases, ties were broken by employing the

279 species having the smallest mean interspecific distance among all nearest
280 neighbours for a given target species. Scatterplots displaying $\log_{10}$-
281 transformed probabilities for all examined species were generated using the
282 *ggplot2* R package ***(36)***. This transformation was selected to aid overall
283 visualization of the difference between p_x and q_x versus p_x' and q_x' by reducing
284 any skewness inherent in the data. In cases where corresponding (p_x, q_x) and
285 (p_x', q_x') pairs were equal to zero on the untransformed scale, resulting in
286 infinite values on the $\log_{10}$ scale, observations were replaced by a large
287 negative number (here, -5) prior to plotting. Following this, the number of
288 species displaying zero values was then indicated.
289
290 **Statistical Interpretation, Notes and Caveats**
291 Calculated values of the proposed statistics and other important
292 quantities can be found in **Table 2**.
293 A defining characteristic of metrics (1) and (2) is their asymmetric
294 *directionality* with respect to intraspecific and interspecific distribution
295 overlap (as well as those for target species and their closely aligned relatives).
296 This is akin to measuring the Kullback-Leibler (KL) divergence ***(37)*** between
297 two probability distributions *P* and *Q*: the distance between *P* and *Q* is not
298 necessarily equal to the distance between *Q* and *P*. When no DNA barcode gap

299 is observed for a species, the extent of overlap will be different depending on
300 whether one is looking at intraspecific or interspecific distances. Note, p_x and
301 q_x are informative in comparison to p_x' and q_x' because computed probabilities
302 reveal the extent to which the distribution of nearest neighbours differs from
303 the genus as a whole.

304 The newly described statistics can be employed in several ways. Firstly,
305 the proposed quantities can be utilized to assess gene marker efficacy for
306 specimen identification: markers attaining lower values of the proposed
307 metrics are preferable as DNA barcoding loci to those displaying higher
308 values, provided selected markers reflect relevant species' histories. Such
309 behaviour would occur in the case where gene markers possess low rates of
310 substitution and display no polymorphism within species; however, it will not
311 solve the problem of incomplete lineage sorting or introgression. Secondly,
312 through coalescent simulations, the defined metrics can be used to assess
313 whether obtained values are consistent with a population-level process
314 having a particular combination of N_e values, mutation rate (μ), dispersal rates
315 (m), and divergence times (τ) as seen in **Figures 1**, **2**, and **Table 1**, and in a
316 similar vein to Yang and Rannala ***(27)***. This agrees well with the universal
317 observation that molecular identifications are significantly hampered when
318 both intraspecific and interspecific distances are below a predefined arbitrary

319 threshold (*e.g.*, the 2% rule ***(1, 2)*** or the 10× rule ***(38)***), which may occur
320 given variable rates of molecular evolution in both taxa and gene markers.
321 However, cautious interpretation should be exercised as these patterns are
322 unlikely to hold strongly in practice for highly speciose groups showing recent
323 adaptive diversification at large spatial scales. In fact, evolutionary processes
324 such as random genetic drift and purifying selection occurring within genes
325 commonly employed in studies of speciation effectively cancel out traces of
326 intraspecific variation over short timeframes. However, such a pattern is less
327 likely to be a problem for neutral mitochondrial loci, but exceptions have been
328 described (*e.g.,* ***(39)***).

329 In comparing results for *Agabus* across sequenced markers for
330 examined taxa, several findings are noteworthy.

331 [**Table 2** near here]

332 Overall, results point to COI-5P being the most suitable gene marker for
333 species delimitation using DNA barcodes in this group, followed by COI-3P.
334 CYTB was found to perform poorly as a DNA barcode for diving beetles,
335 whereas species coverage, albeit still poor, was 21.6% (43/199) and 18.1%
336 (36/199) for COI-5P and COI-3P, respectively. Two equally important factors
337 complicate accurate estimation of DNA barcode gaps, and therefore optimal
338 selection of genomic markers for unambiguous specimen identification: the

number of sampled specimens per species in a genus, and the number of species in the genus. While the COI-5P dataset comprised more species, that for COI-3P contained a larger number of specimens, suggesting these two crucial elements are difficult to balance in tandem. This can be seen through examining the 95% bootstrap percentile intervals for $\bar{p}_x$, $\bar{q}_x$, $\bar{p}_x'$, and $\bar{q}_x'$, which are all quite wide in most cases, meaning there is considerable uncertainty as to their true population means, given poor sampling of taxon genetic diversity. Results overall point to considerable overlap between target species of interest and all other taxa within a given genus. For example, computed mean probabilities for all loci in the q_x, p_x', and q_x' directions differed by an order of magnitude (**Table 2**). This finding suggests that the proposed metrics have sufficient discriminatory power to detect DNA barcode gaps. In comparing intraspecific and interspecific differences, values of p_x were found to all be equal to one (COI-5P; 43 species; COI-3P: 36 species; CYTB: two species), indicating complete overlap of the intraspecific distributions with interspecific distributions, and hence no evidence of DNA barcode gaps across all three assessed genes. A probability of one will always occur whenever a minimum interspecific distance of zero is found. In contrast, much less, but still significant, overlap was noted in the q_x direction, ranging from 5.191×10^{-5} (7 species: *A. bifarius*, *A. biguttatus*, *A. brunneus*,

A. conspersus, *A. discolor*, *A. pallens*, and *A. setulosus*) to 0.1759 (*A. thomsoni*) for COI-5P, 0.0030 (4 species: *A. alexandrae*, *A. binotatus*, *A. clypealis*, and *A. faldermanni*) to 0.3175 (*A. ambiguus*) for COI-3P, and 0.0100 (*A. nevadensis*) to 1 (*A. bipustulatus*) for CYTB, leading to similar conclusions regarding the presence (or lack thereof) of DNA barcode gaps; however, this depended strongly on the locus being considered (**Table 2**; **Figure 3**). In comparing target taxa to their closest conspecifics for all assessed loci, values of p_x' for COI-5P ranged from zero (21 species: *A. ajax*, *A. anthracinus*, *A. audeni*, *A. bicolor*, *A. bifarius*, *A. biguttatus*, *A. brunneus*, *A. colymbus*, *A. conspersus*, *A. crassipes*, *A. didymus*, *A. discolor*, *A. erichsoni*, *A. infuscatus*, *A. labiatus*, *A. moestus*, *A, nebulosus*, *A. pallens*, *A. sturmii*, *A. uliginosus* and *A. undulatus*) to one (eight species: *A. clavicornis*, *A. clypealis*, *A. congener*, *A. inscriptus*, *A. lapponicus*, *A. serricornis*, *A. setulosus*, and *A. thomsoni*), whereas those for q_x' ranged from zero (21 species, same as above) to 0.3922 (*A. thomsoni*). Similarly, values of p_x' for COI-3P ranged from zero (20 species: *A. affinis*, *A. alexandrae*, *A. amoenus*, *A. aubei*, *A. bipustulatus*, *A. cephalotes*, *A. clypealis*, *A. didymus*, *A. disintegrates*, *A. faldermanni*, *A. fulvaster*, *A. lapponicus*, *A. melanarius*, *A. pseudoclypealis*, *A. serricornis*, *A. sturmii*, *A. tristis*, *A. uliginosus*, *A. undulatus*, and *A. unguicularis*) to one (10 species: *A. binotatus*, *A. brunneus*, *A. congener*, *A. glacialis*, *A. guttatus*, *A. heydeni*, *A. labiatus*,

379 *A. ramblae*, *A. rufulus*, and *A. zimmermanni*) and those for q_x' spanned zero (20
380 species, same as above) to 0.2230 (*A. ambiguus*). In the case of CYTB, all
381 values of p_x' and q_x' were identical to those of p_x and q_x since only two species
382 were sequenced. Based on these findings, 21/43 (48.8%) species, 20/36
383 (55.5%) species, and 0/2 (0%) show evidence of a DNA barcode gap for COI-
384 5P, COI-3P, and CYTB, respectively. It is interesting to note that while
385 calculated means of q_x, p_x' and q_x' point to COI-5P being superior to all other
386 examined genetic loci in terms of identification performance, since they attain
387 the smallest values (as would be expected in animal DNA barcoding studies),
388 the above results point to COI-3P instead. This reinforces the tradeoff between
389 balancing the number of specimens sampled for a given species, and the
390 number of species included within a target genus, as well as the fact that DNA
391 barcoding has been one-sided. Results for p_x‘ and q_x‘ compared to p_x and q_x
392 make intuitive sense since the genus-level distribution of pairwise differences
393 encompasses a mixed distribution comprising closely- and more distantly-
394 related species. Findings outline here suggest the above species may warrant
395 further DNA barcode scrutiny, due in part to *Agabus*’ difficult morphology and
396 widespread Holarctic range hampering successful classification in certain
397 cases ***(13)***. For instance, a large degree of overlap between intraspecific and
398 interspecific distributions (as well as those for target species and their closest

neigbours) could be evidence for a recent evolutionary origin, species hybridization, or mitochondrial introgression. Thus, DNA barcoding will fail to discriminate species displaying such patterns.

A potentially useful tool to visualize values of *p*' *and q*' computed for all species' neighbours across all assessed genetic markers is the heatmap, where colour intensity is directly proportional to the magnitude of calculated probabilities. In this way, generated heatmaps can be employed as "look-up tables" to better gauge intraspecific and interspecific distribution overlap for specific pairs of species of interest (and not just the closest neighbour) to a given study. Preliminary investigation has shown this type of visualization to be revealing, particularly when species are not well separated based on plots like **Figure 3**; thus, they will be included in future work.

It seems only one similar methodology for DNA barcode marker selection has been proposed before: the probability of correct identification (PCI) ***(40, 41)***. However, this statistic has not gained wide traction in the DNA barcoding community, appearing to be employed only for Fungi ***(42)***, and is further based purely on statistical, and not coalescent, theory ***(12)***. The PCI employs jackknife resampling of a binomially distributed random variable to obtain estimates of standard error and confidence intervals of specimen identification success with and without the influence of PCR failure ***(12*, 41*)***.

An approach that has seen a much larger body of research as a species delimitation tool for both sexually- and asexually-reproducing organisms is the so-called K/θ ratio ***(43, 44, 45, 46, 47, 48, 49)***. It measures average pairwise sequence differences between clade pairs (K) *versus* said differences found within a clade (θ). If $K/\theta \geq 4$ (the so-called "4× rule"), lineages belong to distinct species with at least 95% probability based on Rosenberg's index of reciprocal monophyly ***(50)***. Unlike the PCI, it appears K/θ has not seen adoption within the DNA barcoding community-at-large, despite showing promise for DNA barcode gap detection ***(12, 47)***. It is stressed that the approach here is simpler than the abovementioned ones and also overcomes the need for order statistics in the case of Phillips *et al.* ***(12)***, as our metrics are easily summarized as simple arithmetic means with well-defined sampling distributions in the limit as sample sizes increase. However, indices discussed here are not the only ones possible, and others should be explored. Problems may arise when multiple curve intersection points or when missing/zero genetic distance values are present. Hence, more sophisticated techniques such as data interpolation, kernel smoothing, local regression, numerical integration, or data transformation may be required. Statistical frameworks like mixture models may also be worth exploring. While our method demonstrates that DNA barcoding has been a one-sided argument, it must be

stressed that obtained estimates likely do not mirror ground truth, since calculated probabilities are based on small taxon sample sizes, making pairwise distance distributions difficult to estimate in practice. A recent article by De Sanctis *et al.* ***(51)*** presents a coalescent theory simulation framework to examine accuracy of taxonomic binning in query sequences to references found within curated genomic databases. This approach may additionally prove informative in introducing greater theoretical rigor into DNA barcoding for molecular species identification purposes.

Conclusion

Here, we characterize the DNA barcode gap using the multispecies coalescent through proposing a suite of easily computed and interpreted nonparametric estimators inspired by population genetics theory along with observed trends in taxon DNA sequence diversity. Application to the beetle genus *Agabus* demonstrates the promise of the proposed statistical metrics for DNA barcode locus selection. The present approach, while having a strong basis in coalescent theory, is ideally suited to addressing applied research questions pertaining to DNA-based specimen identification, such as those encountered in studies of seafood fraud and invasive pest management using techniques like environmental DNA (eDNA)-based targeted species detection and metabarcoding, in addition to characterizing interspecific sequence

diversity. While our metrics are simple, incorporating other coalescent approaches is worthwhile, as is research integrating sample size estimation with tools like *HACSim* (Haplotype Accumulation Curve Simulator) ***(52)***. These are left for future studies.

Author Contributions

J.D.P., C.K.G., and R.G.Y. derived and coded the DNA barcode gap coalescent metrics, analyzed and interpreted the data, generated figures, and wrote the manuscript. N.H. and R.H.H. provided insight on DNA barcoding and other applications of the present work. All authors commented on and approved the final version.

Data Accessibility

FASTA files and R code can be found on GitHub at https://github.com/jphill01/DNA-Barcode-Gap-Coalescent.

Acknowledgements

We sincerely thank Rob DeSalle for the invitation to contribute to this important volume. We acknowledge that the University of Guelph resides on the ancestral lands of the Attawandaron people and the treaty lands and territory of the Mississaugas of the Credit. We recognize the significance of the Dish with One Spoon Covenant to this land and offer our respect to our Anishinaabe, Haudenosaunee and Métis neighbours as we strive to strengthen our relationships with them.

Figures

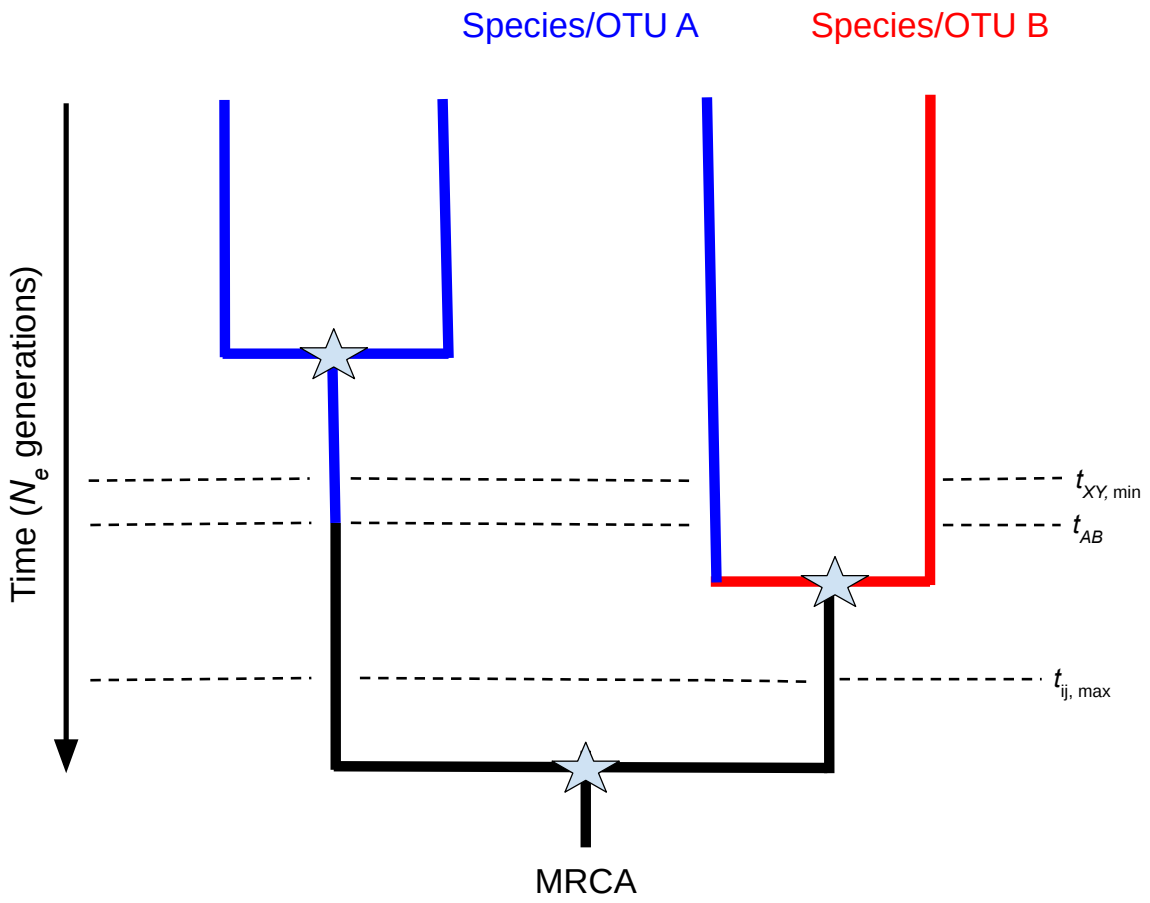
Species/OTU A
Species/OTU B
Time (N_e generations)
$t_{XY,\ min}$
t_{AB}
$t_{ij,\ max}$
MRCA

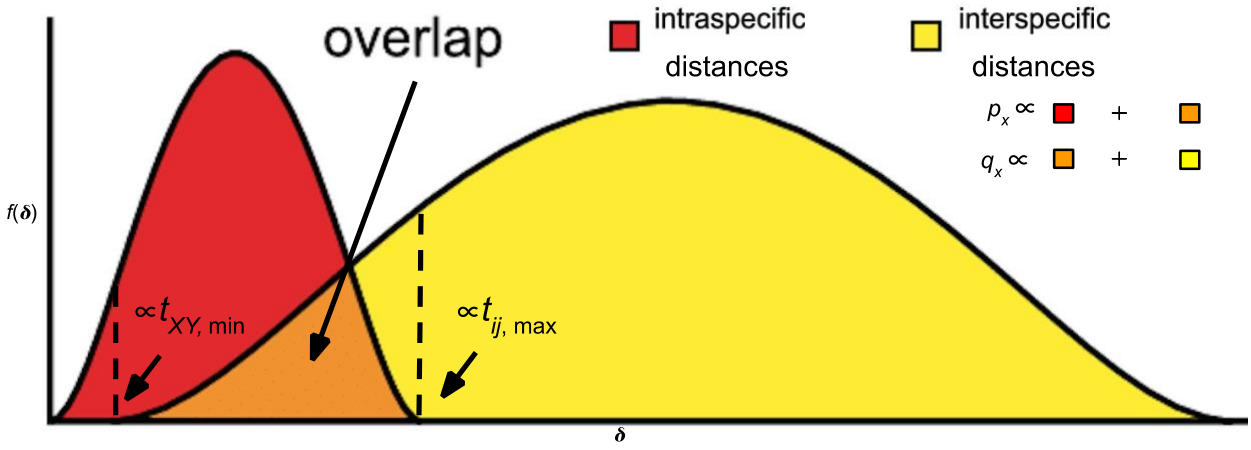
overlap
intraspecific distances
interspecific distances
$p_x \propto$ +
$q_x \propto$ +
$f(\delta)$
$\propto t_{XY,\ min}$
$\propto t_{ij,\ max}$
δ

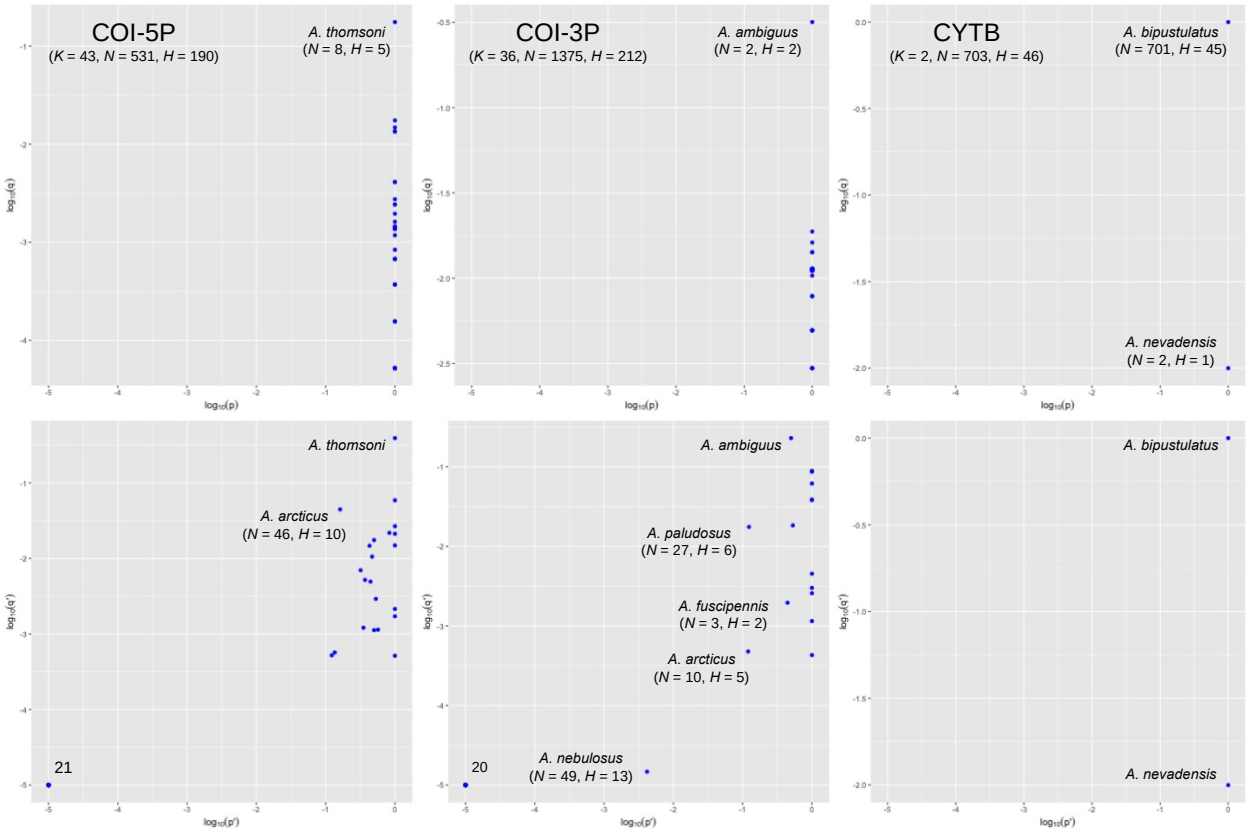

Figure Captions

Figure 1. Multispecies coalescent tree depicting a coalescence history for two species/OTUs and four sampled individuals of a given genus backwards in time to the Most Recent Common Ancestor (MRCA). A case of incomplete lineage sorting is depicted, where species/OTU *A* is paraphyletic to species/OTU *B.* Indicated divergence times are also shown.

Figure 2. Graphical depiction (modified from (7)) of the DNA barcode gap metrics, for a single hypothetical species/OTU *x* with genetic distances δ. Note that distribution overlap (orange area) is implicitly accounted for in the calculation of p_x and q_x. Similar visualizations can be generated for both p_x', and q_x'.

Figure 3. Plots of p_x and q_x for all assessed *Agabus* species on the $\log_{10}(x)$ scale across three mitochondrial loci calculated using *p*-distance. **Top**: Intraspecific *vs*. genus-level comparisons. **Bottom**: Target species *vs*. nearest neighbour comparisons.

564 **Tables**

Parameter	Definition	Range
K	Number of identified species/OTUs within a genus of interest	$(0, \infty)$
$t_{XY,\,min}$	Minimum divergence time within the genus or set of sister species	$(0, \infty)$
$t_{ij,\,max}$	Maximum divergence time within the genus or set of sister species	$(0, \infty)$
t_{AB}	Divergence time between species/OTUs *A* and *B* within the genus	$(0, \infty)$
δ_x	Pairwise genetic distances for all sampled specimens for species *x* within the genus or set of sister species	[0, 1]
$f(\delta_x)$	Distribution of all pairwise genetic distances for all specimens of species *x* within the genus or set of sister species	[0, 1]
$f(d_{ij,\,x})$	Distribution of intraspecific genetic distances for species *x* within the genus or set of sister species	[0, 1]
$f(d_{XY})$	Distribution of interspecific genetic distances for the **entire** genus or set of sister species	[0, 1]
p_x	Proportional overlap of $f(d_{ij}, x)$ with $f(d_{XY})$	[0, 1]
q_x	Proportional overlap of $f(d_{XY})$ with $f(d_{ij,\,x})$	[0, 1]
p_x'	Proportional overlap of $f(d_{ij,\,x'})$ with $f(d_{XY})$ for nearest neighbour species *x*' within the genus	[0, 1]
q_x'	Proportional overlap of $f(d_{XY})$ with $f(d_{ij,\,x'})$ for nearest neighbour species *x*' within the genus	[0, 1]

565

Marker	L	N	H	K	$\overline{p}$	$\overline{q}$ (95% CI)	$\overline{p}'$ (95% CI)	$\overline{q}'$ (95% CI)
COI-5P	600	531	190	43	1	0.0064 (0.0015, 0.0151)	0.3195 (0.2055, 0.4382)	0.0152 (0.0035, 0.0354)
COI-3P	600	1375	212	36	1	0.0180 (0.0085, 0.0360)	0.3256 (0.1868, 0.4745)	0.0165 (0.0051, 0.0325)
CYTB	342	703	46	2	1	0.5050 (0.0100, 1.0000)	1	0.5050 (0.0100, 1.0000)

Table Captions

Table 1. Coalescent DNA barcode gap model parameters, definitions and ranges. Ranges are indicated using interval notation, where parentheses and brackets signify open and closed intervals respectively.

Table 2. Calculated DNA barcoding gap statistics using *p*-distance for several sequenced mitochondrial loci in *Agabus* considering only species with at least two specimens. ***L*** is the alignment length in basepairs. ***N*** is the number of sequences used to compute the pairwise genetic distance matrix. ***H*** is the number of unique haplotypes.

References

1. Hebert P.D.N., Cywinska A., Ball S.L., and deWaard J.R. (2003a). Biological identifications through DNA barcodes. *Proceedings of the Royal Society of London B: Biological Sciences,* **270**, 313–321.

2. Hebert, P.D.N., Ratnasingham, S., and deWaard, J.R. (2003b). Barcoding animal life: cytochrome *c* oxidase subunit 1 divergences among closely related species. *Proceedings of the Royal Society of London B* (**Suppl. 1**), S96-S99.

3. Ballard, J.W.O. and Rand, D.M. (2005). The population biology of mitochondrial DNA and its phylogenetic implications. *Annual Reviews of Ecology, Evolution, and Systematics*, **36**: 621-642.

4. Phillips, J.D., Gillis, D.J., and Hanner, R.H. (2019). Incomplete estimates of genetic diversity within species: Implications for DNA barcoding. *Ecology and Evolution,* **9**: 2996-3010.

5. Ratnasingham S. and Hebert P.D.N. (2007) Bold: The barcode of life data system (http://www.barcodinglife.org). *Molecular Ecology Notes,* **7**, 355–364.

6. Zhang, A.B., He, L.J., Crozier, R.H., Muster, C., and Zhu, C.-D. (2010). Estimating sample sizes for DNA barcoding. *Molecular Phylogenetics and Evolution*, **54**: 1035-1039.

7. Meyer C.P. and Paulay, G. (2005). DNA barcoding: Error rates based on comprehensive sampling. *PLOS Biology*, **3**: e422.

8. Meier, R., (2008). The use of mean instead of smallest interspecific distances exaggerates the size of the "barcoding gap" and leads to misidentification. *Systematic Biology*, **57**: 809-813.

9. Dasmahapatra, K.K., Elias, M., Hill, R.I., Hoffman, J.I, and Mallet, J. (2010). Mitochondrial DNA barcoding detects some species that are real, and some that are not. *Molecular Ecology Resources*, **10**, 254-273.

10. Hickerson, M.J., Meyer, C.P., and Moritz, C. (2006). DNA barcoding will often fail to discover new animal species in broad parameter space. *Systematic Biology*. **55**, 729–739.

11. Stoeckle M.Y. and Thaler D.S. (2014). DNA barcoding works in practice but not in (neutral) theory. *PLOS ONE,* **9**, e100755.

12. Phillips, J.D., Gillis, D.J., and Hanner, R.H. (2022). Lack of statistical rigor in DNA barcoding likely invalidates the presence of a true species' barcode gap. *Frontiers in Ecology and Evolution*, **10**: 859099.

13. Bergsten, J., Bilton, D.T., Fujisawa, T., Elliott, M., Monaghan, M.T., Balke, M., Hendrich, L., Geijer, J., Herrmann, J., Foster, G.N., Ribera, I., Nilsson, A.N., Barraclough, T.G., and Vogler, A.P. (2012). The effect of geographical scale of sampling on DNA barcoding. *Systematic Biology*, **61**: 851-869.

14. Matz, M. and Nielsen, R. (2005). A likelihood ratio test for species membership based on DNA sequence data. *Philosophical Transactions of the Royal Society of London B: Biological Sciences*, **360**: 1969-1974.

15. Nielsen, R. and Matz, M. (2006). Statistical approaches for DNA barcoding. *Systematic Biology*, **55**: 162-169.

16. Pons, j., Barraclough, T., Gomez-Zurita, J., Cardoso, A., Hazell, S., Kamoun, S., Sumlin, W.D., and Vogler, A.P. (2006). Sequence-based species delimitation for the DNA taxonomy of undescribed insects. *Systematic Biology*, **55**: 585-609.

17. Puillandre, N., Lambert, A., Brouillet, S., and Achez, G. (2011). ABGD, Automatic Barcode Gap Discovery for species delimitation. *Molecular Ecology*, **21**: 1864-1877.

18. Zhang, J., Kapli, P., Pavlidis, P., and Stamatakis, P. (2013). A general species delimitation method with applications to phylogenetic placements. *Bioinformatics*, **29**: 2869-2876.

19. Ratnasingham, S. and Hebert, PDN (2013) A DNA-based registry for all animal species: The Barcode Index Number (BIN) system. *PLOS ONE*, **8**, e66213.

20. Puillandre, N. Brouillet, S. and Achez, G. (2021). ASAP: assemble species by automatic partitioning. *Molecular Ecology Resources*, **21**: 609-622.

21. Ezard, T., Fujisawa, T., and Barraclough, T. (2017). splits: Species LImits by Threshold Statistics. R package version 1.0.

22. Eckert, E.M., Fontaneto, D., Coci, M., and Callieri, C. (2015). Does a barcoding gap exist in prokaryotes? Evidences from species delimitation in cyanobacteria. *Life*, **5**: 50-64.

23. Zimmerman, J., Jahn, R., and Gemeinholzer, B. (2011). Barcoding diatoms: evaluation of the V4 subregion on the 18S rRNA gene, including new primers and protocols. *Organisms Diversity and Evolution*, **11**: 1-20.

24. Kingman, J.F.C. (1982). The coalescent. *Stochastic Processes and Their Applications*, **13**: 235-248.

25. Hubert, N. and Hanner, R. (2015) DNA barcoding, species delineation and taxonomy: a historical perspective. *DNA Barcodes*, **3**: 44-58.

669 26. Rannala B and Yang Z. (2003). Bayes estimation of species divergence
670 times and ancestral population sizes using DNA sequences from multiple loci.
671 *Genetics*. **164**: 1645–1656.
672
673 27. Yang, Z. and Rannala, B. (2017). Bayesian species identification under the
674 multispecies coalescent provides significant improvements to DNA barcoding
675 analyses. *Molecular Ecology*, **26**: 3028-3036.
676
677 28. Collins, R.A. and Cruickshank. R.H. (2014). Known knowns, known
678 unknowns, unknown unknowns and unknown knowns in DNA barcoding: a
679 comment on Dowton et al. *Systematic Biology*, **63**: 1005-1009.
680 29. Jukes, T.H. and Cantor, C.R. (1969) Evolution of Protein Molecules. In:
681 Munro, H.N., Ed., Mammalian Protein Metabolism, Academic Press, New York,
682 21-132.
683
684 30. Kimura, M. (1980). A simple method for estimating evolutionary rates of
685 base substitutions through comparative studies of nucleotide sequences.
686 *Journal of Molecular Evolution*, **16**: 111-120.
687 31. Efron, B. (1979). Bootstrap methods: another look at the jackknife. *The*
688 *Annals of Statistics*, **7**: 1-26.
689
690 32. Young, RG, Gill, R, Gillis, D., and Hanner, RH (2021) Molecular Acquisition,
691 Cleaning and Evaluation in R (MACER) – A tool to assemble molecular marker
692 datasets from BOLD and GenBank. *Biodiversity Data Journal*, **9**, e71378.
693 33. R Core Team (2022). R: A language and environment for statistical
694 computing. R Foundation for Statistical Computing, Vienna, Austria. URL
695 https://www.R-project.org/.
696 34. Canty, A. and Ripley, B. (2021). boot: Bootstrap R (S-Plus) Functions. R
697 package version 1.3-28.
698 35. Davison, A. C. and Hinkley, D. V. (1997). Bootstrap Methods and Their
699 Applications. Cambridge University Press, Cambridge.
700
701 36. Wickham, H. ggplot2: Elegant Graphics for Data Analysis. Springer-Verlag
702 New York, 2016.

703 37. Kullback, S. and Leibler, R. (1951). On information and sufficiency. *Annals*
704 *of Mathematical Statistics*, 22: 49-86.
705
706 38. Hebert, P.D.N., Stoeckle, M.Y., Zemlak, T.S., and Francis, C.M. (2004).
707 Identification of Birds through DNA barcodes. *PLOS Biology*, **2**: e312.

708 39. D'Ercole, J., Dapporto, L., Schmidt, B.C., Dincă, V., Talavera, G., Vila, R., and
709 Hebert, P.D.N. (2022). Patterns of DNA barcode diversity in butterfly species
710 (Lepidoptera) introduced to the Nearctic. *European Journal of Entromology*,
711 119: 379-387.

712
713 40. Martin, M.P., Daniëls, P.P, Erickson, D., and Spouge, J.L. (2020). Figures of
714 merit and statistics for detecting faulty species identification with DNA
715 barcodes: a case study in *Ramaria* and related fungal genera. *PLOS ONE*, **15**:
716 e0237507
717
718 41. Spouge, J. and Mariño-Ramirez, L. (2012). The practical evaluation of DNA
719 barcode efficacy. In: *DNA Barcodes: Methods and Protocols*. W.J. Kress and D.L
720 Erickson, eds. *Springer*.
721
722 42. Suwannasai, N., Martin, M.P., Phosri, C., Sihanonth, P., Whalley, A.J.S., and
723 Spouge, J.L. (2013). Fungi in Thailand: A case study of the efficacy of an ITS
724 barcode for automatically identifying species within the Annulohypoxylon and
725 Hypoxylon genera. *PLOS ONE*, **8**: e54529.
726
727 43. Birky, C.W.J, Wolf, C., Maughan, H., Herbertson, L., and Henry, E. (2005).
728 Speciation and selection without sex. *Hydrobiologia* **546**: 29–45.
729
730 44. Birky C.W.J. and Barraclough T.G. (2009). Asexual Speciation. In: Schon, I.,
731 Martens, K., van Dijk, P., eds. Lost Sex. New York: Springer. pp. 201–216.
732
733 45, Birky, C.W.J., Adams, J., Gemmel, M., and Perry, J. (2010). Using population
734 genetic theory and DNA sequences for species detection and identification in
735 asexual organisms. *PLOS ONE*, **5**: e10609.
736
737 46. Birky, C.W.J., Ricci, C., Melone, G., and Fontaneto, D. (2011). Integrating
738 DNA and morphological taxonomy to describe diversity in poorly studied
739 microscopic animals: new species of the genus *Abrochtha* Bryce, 1910
740 (Rotifera: Bdelloidea: Philodinavidae). *Zoological Journal of the Linnean*
741 *Society*, 161: 723–734.

47. Birky, C.W.J. (2013) Species detection and identification in sexual organisms using population genetic theory and DNA sequences. *PLOS ONE*, **8**: e52544.

48. Birky, C. W.J. and H. Maughan (2020). Evolutionary genetic species detected in prokaryotes by applying the K/θ ratio to DNA sequences. *bioRxiv*. https://www.biorxiv.org/content/10.1101/2020.04.27.062828v3.full

49. Spöri, Y. Stoch, F., Dellicour, S., Birky, C.W.J., and Flot, J.-F. (2021). KoT: an automatic implementation of the K/θ method for species delimitation. *biorXiv*. *https://www.biorxiv.org/content/10.1101/2021.08.17.454531v2*

50. Rosenberg, N. (2007). Statistical tests for taxonomic distinctiveness from observation of monophyly. *Evolution*, **61**: 317-323.

51. De Sanctis, B., Money, D., Winther Pedersen, M., and Durbin, R. (2021). A theoretical analysis of taxonomic binning accuracy. *Molecular Ecology Resources*, **22**: 2208-2219.

52. Phillips, J.D., French, S.H., Hanner, R.H., and Gillis, D.J. (2020). HACSim: An R package to estimate intraspecific sample sizes for genetic diversity assessment using haplotype accumulation curves. *PeerJ Computer Science*, **6**: 1-37.